Catalysis Today 178 (2011) 79–84

Contents lists available at SciVerse ScienceDirect

Catalysis Today

journal homepage: www.elsevier.com/locate/cattod

The effect of support and synthesis method on the methanation activity of alumina-supported cobalt–ruthenium–lanthana catalysts

Esther Kok[a], Noel Cant[a], David Trimm[a,b], Jason Scott[a,*]

[a] ARC Centre of Excellence for Functional Nanomaterials, School of Chemical Engineering, The University of New South Wales, Sydney, NSW 2052, Australia
[b] CSIRO Earth Science and Resource Engineering, Clayton, Vic 3168, Australia

ARTICLE INFO

Article history:
Received 30 April 2011
Received in revised form 1 September 2011
Accepted 1 September 2011
Available online 7 October 2011

Keywords:
Cobalt
Ruthenium
Lanthanum
Impregnation
Alumina
Methanation

ABSTRACT

The effect of alumina support source as well as preparation method on the methanation activity of cobalt catalysts promoted with lanthanum and ruthenium was investigated. The catalysts were prepared by incipient wetness impregnation using either an acetone and ethanol mix (ratio 4:1 – non-aqueous) or using a dilute nitric acid solution (aqueous) on two commercial aluminas, Puralox SBA200 or Norton type SA6176 alumina. The catalysts were characterised by nitrogen adsorption/desorption, X-ray diffraction, temperature-programmed reduction, temperature-programmed desorption of hydrogen and Fourier transform infrared spectroscopy. Both the support and synthesis method were found to influence the methanation activity with the non-aqueous plus Puralox combination giving the best performance. The activity differences could arise from modification of surface properties leading to variations in cobalt crystallite size and hence improved cobalt metal dispersion.

1. Introduction

Cobalt is considered one of the most active metals for synthesis gas – carbon monoxide plus hydrogen – reactions [1–4]. Cobalt catalyst activity is reported to be influenced by a number of factors, such as support [5,6], additives [7–11] and the number of active sites formed by reduction. The active site density is governed by Co° crystallite size, Co° dispersion and the degree of reduction [12–14]. The chemical properties of the support also play a role in influencing the catalytic activity primarily through modifying the reducibility and dispersion of cobalt [15,16]. Synthesizing highly dispersed Co catalysts often requires a strong interaction between the support and Co metal; however this may be to the detriment of catalyst activity. Strong interaction between the metal and support generally lower the extent of reduction and/or may leave a fraction of the cobalt chemically inactive after reduction [17–19]. Catalyst synthesis conditions play a significant role in controlling this interaction. Solvents used to either dissolve the Co precursor or pretreat the support can influence the interaction between cobalt and the support. This may arise from alkyl groups in the solvent remaining on the support surface and reducing sintering of the supported cobalt [16,20]. For example, Ho et al. reported that impregnation involving an ethanol and cobalt nitrate mixture instead of aqueous cobalt nitrate improved cobalt catalyst dispersion and retained a high extent of reduction of the cobalt phase [21]. Several groups have observed that the pH value of the precursor solution can also alter the interaction between cobalt and the support, providing variations in dispersion and reducibility of the supported cobalt which in turn strongly impacted on the catalytic performance [15,22,23].

This work compares the effect of ethanol and acetone mixed impregnation on two γ-aluminas with that of nitric acid and water impregnation in terms of cobalt crystallite size, cobalt dispersion, degree of reduction and methanation activity.

2. Experimental

2.1. Catalyst preparation

Two γ-alumina substrates (Norton type SA6176, grain size 60–71 μm; Puralox SBA 200, grain size 51 μm) were used as catalyst supports in this work. The alumina supports were initially loaded with lanthana after which Co and Ru were simultaneously added. These components were added under either aqueous or non-aqueous conditions.

2.1.1. Aqueous

Lanthanum (1 wt%) was initially loaded onto the γ-alumina using aqueous lanthanum nitrate (Aldrich, 99.99%). Briefly, 2 g of alumina support was suspended in ~10 ml of lanthanum nitrate

* Corresponding author. Tel.: +61 2 9385 7966; fax: +61 2 9385 5966.
E-mail address: jason.scott@unsw.edu.au (J. Scott).

0920-5861/$ – see front matter © 2011 Elsevier B.V. All rights reserved.
doi:10.1016/j.cattod.2011.09.015

solution at pH 2 (adjusted using 3 M nitric acid) and agitated for 3 h. The slurry was then dried for 12 h in an oven at 120 °C after which it was calcined at 400 °C for 8 h. Lanthanum was used as an additive in this work as it was previously demonstrated to improve Co dispersion and catalyst performance for methanation [24]. Promotion with cobalt (20 wt%) and ruthenium (0.43 wt%) the La/γ-alumina was achieved by co-impregnation of cobalt nitrate (Sigma–Aldrich, 98+%) and ruthenium nitrosyl nitrate (Aldrich, 1.5% Ru) precursors. The La/γ-alumina was suspended in approximately 10 ml of the Co/Ru nitrate precursor solution (at pH 2 – adjusted using 3 M nitric acid) under agitation for 3 h and then dried for 12 h in an oven at 120 °C after which it was again calcined at 400 °C for 8 h. A pH of 2 was maintained throughout both impregnation processes by regular addition of nitric acid.

2.1.2. Non-aqueous

Similar to the aqueous preparation, 1 wt% lanthanum was initially loaded onto the γ-alumina using (aqueous) lanthanum nitrate. This was followed by simultaneous non-aqueous promotion with cobalt (20 wt%) and ruthenium (0.43 wt%). Non-aqueous impregnation used an ethanol/acetone (1:4) mixture in place of the nitric acid solution with no pH adjustment. Co/Ru addition was performed using 15 impregnation cycles with 0.2 ml added to the 2 g of La/γ-alumina during each cycle [25]. This was performed while the sample was held at 50 °C. Upon completing precursor addition the sample was ramped at a rate of 1 °C/min to 120 °C whereby it was held for 4 h. The sample was then calcined for 8 h at 400 °C.

2.2. Catalyst characterisation

A Perkin Elmer Optima 7300 inductively coupled plasma optical emission spectrometer (ICP-OES) was used to determine cobalt, lanthanum, ruthenium and sodium content of the catalysts. The amount of metal was measured using a segmented-array, charged coupled device detector. The catalyst sample was digested by the fusion method involving a mixture of lithium metaborate (65%) and lithium tetraborate (35%) prior to analysis for cobalt, lanthanum and ruthenium. When determining sodium content the catalyst sample was extracted with HNO_3.

BET surface area, pore volume and average pore diameter of the catalysts were evaluated by N_2 adsorption at 77 K using a Micromeritics Tristar 3000 instrument. The catalysts were outgassed at 150 °C for 6 h prior to analysis.

The zeta potential of La/γ-alumina for both Puralox and Norton supports at pH 7 and pH 2 were measured by phase analysis light scattering (PALS, Brookhaven BI-90 PALS) using Smoluchowski's theory. Acidic pH adjustment was achieved using 3 M nitric acid.

XRD measurements were carried out on a Philips X'Pert MPD diffractometer fitted with a Cu Kα source and operated with a scan rate of 2.6°/min and a step size of 0.0262°. The average size of the Co_3O_4 crystallites in the calcined catalysts was estimated from the line width using the Scherrer equation. XRD was also used to confirm the presence of Co metal on the catalyst following reduction. This required passivation of the Co metal prior to analysis. Passivation involved passing a stream of 0.5% O_2/He (at 10 ml/min) over the reduced catalyst for 10 h at room temperature.

Fourier transform infrared (FTIR) spectroscopy was performed using a Perkin Elmer Spotlight 400 FTIR Microscope equipped with an attenuated total reflectance (ATR) imaging crystal on the calcined samples. Prior to scanning, each calcined sample was treated for 2 h with a 50 ml/min He stream at 120 °C in a reactor setup. The transmittance spectra were obtained using 500 scans at 4 cm^{-1} resolution at ambient temperature.

Cobalt reducibility over the temperature range 25–800 °C was determined by Temperature Programmed Reduction (TPR) using a Micromeritics Autochem II 2920 instrument. The catalyst was pretreated by first passing 50 ml/min Ar gas through the catalyst bed for 30 min at 300 °C before cooling to room temperature. A 5% H_2/Ar gas stream was then passed through the catalyst bed at 50 ml/min and the temperature ramped at 5 °C/min to 800 °C.

Hydrogen Temperature Programmed Desorption (H_2-TPD) measurements were carried out on the same Micromeritics Autochem II 2920 instrument using 0.18 g samples of catalyst for each analysis. Catalyst pretreatment involved passing 50 ml/min of Ar gas through the catalyst bed for 30 min at 300 °C before cooling to room temperature. The catalyst was then reduced under a 50 ml/min 10% H_2/He gas stream at a temperature of 400 °C for 10 h after which it was cooled under flowing 10% H_2/He to 50 °C. The sample was then held under 50 ml/min of 100% H_2 for 120 min and further cooled with flowing 100% H_2 to 40 °C. The flow was changed to 50 ml/min of Ar and held for 30 min to remove physisorbed and weakly bound H_2. Retained hydrogen was desorbed by increasing the temperature at a ramp rate of 10 °C/min to 350 °C where it was held for 1 h.

Table 1
Elemental composition of catalysts prepared by aqueous and non-aqueous impregnation methods.

Sample	Metal content			
	Co (wt%)	La (wt%)	Ru (wt%)	Na (ppm)
Puralox (P)	–	–	–	37.8
Norton (N)	–	–	–	45.5
Co-P-aq	19.2	0.82	0.34	35.5
Co-N-aq	19.5	0.81	0.36	37.8
Co-P-nonaq	19.4	0.84	0.36	35.7
Co-N-nonaq	19.2	0.84	0.37	38.2

2.3. Catalytic activity

Catalytic tests were performed on 0.2 g samples mounted in a glass tube (6 mm I.D.) fixed bed flow reactor operating at 200 °C and ambient pressure. The thermocouple used to control the temperature of the reactor was located within the catalyst bed. Prior to activity testing, the sample was activated in 50 ml/min of 50% H_2/He from room temperature to 400 °C at a ramp rate of 5 °C/min where it was held for 10 h. The sample was then cooled to 200 °C under He after which the reactant gases (4% CO, 40% H_2 balance helium) were introduced at a flow rate of 50 ml/min. Online gas chromatography analysis, using a Shimadzu GC8A gas chromatograph fitted with a Porapak Q column and a thermal conductivity detector, was used to determine CO and methane levels. Water produced by the reaction was removed by a cold trap located between the reactor and the chromatograph. Activities were measured over a period of 480 min and are expressed in terms of the percentage conversion of CO.

3. Results and discussion

The actual metal loadings for the four calcined catalyst samples are provided in Table 1. All elemental loadings are slightly below the nominal values (20%, 1% and 0.43% for Co, La and Ru, respectively) with the difference similar for each catalyst. Based on the values in Table 1, the maximum surface coverage (monolayer) attainable by lanthana on both the Puralox and Norton alumina supports was estimated to be no greater than ~6–7% implying the loaded La has no discernible impact on the surface charge of the original alumina. This idea was confirmed by zeta potential analysis whereby zeta potentials of both the La–Al_2O_3 and Al_2O_3 supports (at pH 2 and pH 7) were found to lie in the range +36 to +46 mV.

The sodium content of the synthesised catalysts was also evaluated as it has been previously reported to influence catalyst

Table 2
Physical properties of pristine γ-alumina supports and calcined γ-alumina supports promoted with La, Co and Ru.[a]

Sample	S_{BET} (m^2/g)	Pore volume (cm^3/g)	Pore diameter (nm)	XRD Co_3O_4 crystallite size (nm)
Puralox (P)	157	0.42	8.2	–
Norton (N)	234	0.80	11.4	–
Co-P-aq	134	0.26	7.0	8.2
Co-N-aq	195	0.56	9.6	8.3
Co-P-nonaq	121	0.26	7.8	7.3
Co-N-nonaq	173	0.50	10.3	7.6

[a] Included are Co_3O_4 crystallite sizes following calcination. Pore volume and diameter were calculated using the BJH model.

performance for Fischer Tropsch reactions [26]. The difference in the sodium content of the synthesised catalysts for the two supports is small (~2 ppm). To identify whether the sodium originated from the impregnation salts or was originally present in the alumina supports, ICP-OES was performed on the neat alumina samples. The results, as illustrated in Table 1, show the supports possess comparable sodium contents before and after impregnation, indicating the sodium originates from the alumina support with minimal contribution from the metal precursor salts.

Comparison of the BET surface area and pore distributions of the two alumina supports (Table 2) indicates the Norton type SA6176 support has an approximately 50% larger surface area than the Puralox SBA200 support, due primarily to a more open pore structure as reflected by its larger pore volume. Loading the supports with the active components (La, Co, Ru) decreased both the SSA and the pore volume due to partial filling of pores by cobalt oxide crystallites and/or pore collapse due to dissolution of the support during the impregnation process [27]. The capacity for the impregnation solutions to dissolve Al and La was investigated by subjecting the lanthana-loaded alumna supports to the conditions used to load Co and Ru but without the Co and Ru salts present with the results detailed in Table 3. The aqueous impregnation conditions are represented by the values at pH 2 while the non-aqueous impregnation is mimicked by the values at pH 7. The findings show that between 0.83% and 0.88% of the aluminium and 7.3–8.1% of the lanthanum were released into solution under the acidic conditions, depending on the alumina support. At pH 7, no aluminium dissolution was observed while between 1.59% and 2.96% of the lanthanum was released into solution. These findings indicate that, under acidic (aqueous) conditions, pore collapse may occur contributing to the loss in surface area. The milder pH conditions in the non-aqueous environment result in less support dissolution, suggesting the reduction in surface area for this catalyst arises largely through the pores being filled with Co crystallites. Preparation using the non-aqueous method leads to a greater loss in area (~24%) compared with the aqueous method (~15%).

XRD patterns for the calcined samples are shown in Fig. 1. Strong peaks pertaining to Co_3O_4 and alumina reflections were observed with peaks representing lanthanum and ruthenium oxides absent due to their lower concentrations. The widths of the Co_3O_4 peaks, and hence the corresponding average Co_3O_4 crystallite sizes were calculated using the Scherrer equation for the peaks located at $2\theta = 56^\circ$ and 59.5° (4 2 2 and 5 1 1). The values are provided in Table 2 and show both the support and the impregnation environment impact on the Co_3O_4 crystallite size. That is, the non-aqueous impregnation method delivers a smaller Co_3O_4 crystallite size than the aqueous method as does the Puralox support over the Norton support. The difference in Co_3O_4 crystallite size may arise from factors such as impregnation pH, diameter of the support pores and characteristics of the aqueous/non-aqueous impregnation solution as discussed below.

During aqueous impregnation at low pH, the alumina surface is more positively charged making Co/Ru species mobility more amenable due to a lower attraction to the surface. This facilitates larger crystallite formation due to the increased tendency of Co_3O_4 to agglomerate during calcination. For non-aqueous impregnation, the pH is closer to neutral, hence the surface of the alumina is less positive. This promotes stronger interaction between the Co/Ru and the alumina surface and provides a greater number of potential anchoring sites contributing to a smaller Co_3O_4 crystallite size [15,27].

Table 2 indicates the average Co_3O_4 crystallite size was comparable to or smaller than the average pore diameter of both alumina supports. The Puralox support possesses a narrower pore structure compared with the Norton support which may act to constrict the relative Co_3O_4 crystallite sizes for the two supports. That is, the smaller pores in the Puralox support may limit growth of the Co_3O_4 particles to a greater extent than the Norton support [28]. The apparent dependence of the Co_3O_4 particle sizes on the catalyst pore diameters also implies a localisation of Co_3O_4 crystallites in the alumina pores which can contribute to the loss in pore volume and area during impregnation.

The different volatilities of the two dispersing media as well as the variations in impregnation procedures may also influence the Co_3O_4 crystallite size. It is anticipated the non-aqueous solution will evaporate at a faster rate due to both its more volatile nature as well as using multiple cycles of small impregnation volumes

Table 3
Dissolution of aluminium and lanthanum from calcined lanthanum γ-alumina-support using aqueous (pH 2) and simulated non-aqueous (pH 7) preparation conditions.

Sample	Amount of metal in catalyst		Amount of metal dissolved	
	Al (mg/gcat)	La (mg/gcat)	Al (mg/gcat)	La (mg/gcat)
La-P-aq (pH 2)	208.4	8.2	1.73	0.60
La-N-aq (pH 2)	208.4	8.1	1.83	0.66
La-P-nonaq (pH 7)	208.3	8.4	<0.1	0.13
La-N-nonaq (pH 7)	208.3	8.4	<0.1	0.24

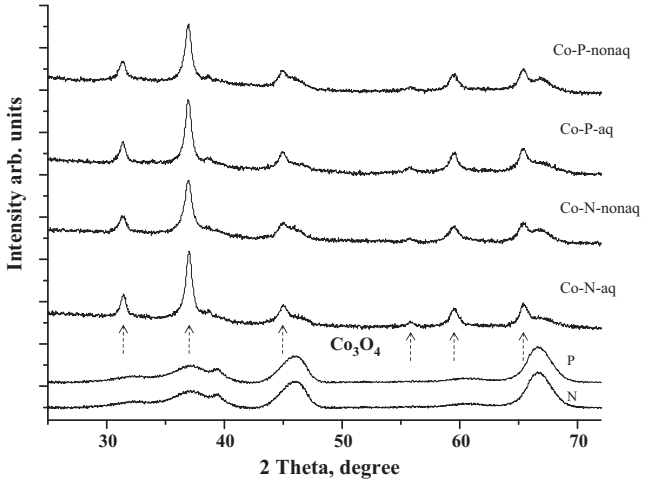

Fig. 1. X-ray diffraction patterns of calcined alumina-supported La/Co/Ru catalysts.

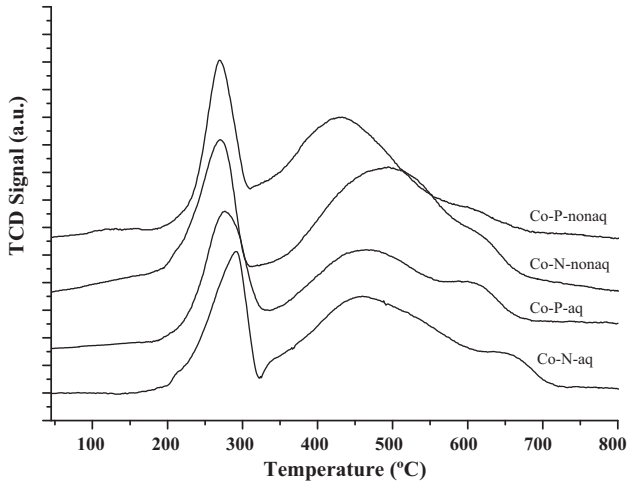

Fig. 2. H_2-TPR profiles of alumina-supported La/Co/Ru catalysts.

compared with the aqueous solution. This will lead to faster saturation of the metal precursors in the impregnating solution in turn promoting a faster precipitation/crystallisation rate which may then lead to a smaller crystallite size [29].

The ease of Co_3O_4 reduction to metallic Co for all calcined catalysts was evaluated using H_2-TPR with the resulting profiles given in Fig. 2. All catalysts displayed three reduction peaks. The first reduction peak occurred over the temperature region 200–325 °C, reflecting the reduction of Co_3O_4 to CoO. The second peak appeared between 325 and 580 °C can be attributed to CoO reduction to metallic Co. The third peak is present as a shoulder on the second peak and occurred at temperatures above 580 °C and may represent difficult to reduce mixed oxide species [30,31]. These mixed oxide species may originate from the dissolution of alumina and lanthana followed by their reprecipitation as Co–Al and/or Co–La composites during the Co/Ru impregnation step. As previously indicated in Table 3, during impregnation lanthanum is released into solution at pH 7 (mimicking the non-aqueous environment) while both lanthanum and aluminium are released into solution at pH 2 (aqueous environment). It is conceivable that these cations may then reprecipitate as mixed cobalt oxides (depending on relative solubilities) during the drying stage.

Of particular interest in the H_2-TPR profiles is the comparative size of the third reduction peak (580 °C) for the two synthesis conditions. This peak is smaller for samples prepared using the non-aqueous precursor than for the aqueous precursor, which may arise from either the lower degree of (La/Al) support dissolution (Table 3) during impregnation as already discussed and/or decreased interaction between the Co and the alumina (or lanthana) during calcination of the non-aqueous catalysts. Decreased interaction may arise from changes to the support surface introduced by the ethanol/acetone impregnation mixture, as identified by FTIR analysis (Fig. 3).

FTIR-ATR analysis of the alumina surface following Co/Ru impregnation by the two methods (Fig. 3) indicated the precursor solution influenced surface chemistry of the support. The peak at 3600–3100 cm^{-1} represents the OH stretching vibration of OH species remaining on the surface after impregnation [32]. In addition, the non-aqueous samples exhibit a peak over the region 1480–1340 cm^{-1}, representing the deformation of CH_2 and CH_3 surface species [33]. This observation reveals acetone and/or ethanol were adsorbed on the alumina surface during non-aqueous impregnation with CH_2 and CH_3 functional groups remaining on the surface even after calcination at 400 °C for 8 h. It is thought that the difference in surface functionality, in particular the presence of organic groups, arising from the impregnation solutions may contribute to a decreased interaction between cobalt and alumina, while still allowing for retention of the smaller Co crystallite size. Ho et al. previously suggested that CH_2 and CH_3 functional groups on an alumina surface hindered the agglomeration of Co_3O_4 by physical interference during the thermal decomposition of cobalt nitrate promoting a smaller Co_3O_4 crystal size [16]. The findings in this work imply the surface hydrocarbons may also interfere with interaction between the Co species and the alumina surface during the calcination process.

The reduction of Co_3O_4 to metallic Co was verified by XRD analysis on passivated catalyst samples. Spectra of the passivated catalysts are given in Fig. 4 and confirm the reduction conditions (50 ml/min of 50% H_2/He from room temperature to 400 °C at a ramp rate of 5 °C/min and held for 10 h) lead to the presence of metallic Co. The peak located at $2\theta = 44.3°$ (1 1 1) is due to Co metal in the cubic form [34], while the peak at 2θ of 45.8° represents CoO [35,36]. All catalysts exhibit similar diffraction patterns indicating a mixture of Co and CoO were present on the passivated samples.

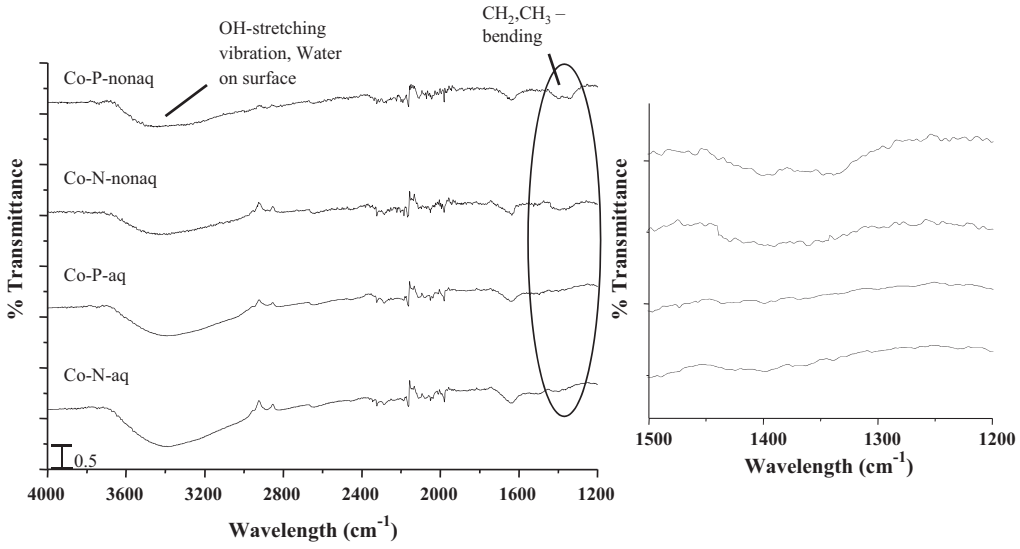

Fig. 3. FTIR-ATR spectra of calcined alumina-supported La/Co/Ru catalysts following pretreatment at 120 °C in He for 2 h.

Table 4
Cobalt crystallite size and cobalt dispersion taken from XRD and H_2-TPD analyses for alumina-supported La/Co/Ru catalysts.

Catalyst	Co crystallite size (nm)		H_2-TPD results		
	Co from XRD[a]	Co from Co_3O_4 size[b]	H_2 desorbed mol (H) $g^{-1} \times 10^{-4}$	% Dispersion	Co° diameter (nm)[c]
Co-P-aq	6.5	6.1	2.51	7.6	6.6
Co-N-aq	6.9	6.2	2.31	6.6	7.5
Co-P-nonaq	5.3	5.5	2.93	8.6	5.8
Co-N-nonaq	5.8	5.9	2.76	8.1	6.1

[a] Calculated from the line widths at $2\Theta = 44.3°$ using the Scherrer equation.
[b] Calculated from the Co_3O_4 sizes in Table 2 assuming reduction to metal reduces the crystallite size by a factor of 0.75 [32].
[c] Calculated from Co dispersion values assuming the crystallites are uniform spheres.

Similar to the XRD findings for the calcined samples (Table 2), catalysts fabricated by the non-aqueous process and then reduced gave a smaller crystallite size than for the aqueous process, with the values listed in Table 3. It has been reported that the metallic Co crystallite size can be estimated from the Co_3O_4 crystallite size by multiplying the Co_3O_4 values by a factor of 0.75 [37]. Table 4 shows good agreement in relation to metallic Co crystallite sizes for the four catalysts when comparing the adjusted Co_3O_4 XRD values using this factor with the actual metallic Co XRD values.

Co metal dispersion values of the reduced catalysts, as measured using H_2-TPD, are provided in Table 4. Note that control experiments demonstrated hydrogen uptake by the γ-alumina supports was negligible. The findings indicate catalysts prepared by the non-aqueous method desorb relatively larger amounts of hydrogen than the aqueous catalysts. This translates to a relative increase in Co metal dispersion of 13% on the Norton γ-alumina support and 23% on the Puralox γ-alumina support for the non-aqueous synthesis method. Moreover, estimation of the Co crystallite sizes from the H_2-TPD results (Table 4) confirms the XRD findings in relation to the influence of impregnation solution on Co crystallite size.

Bae et al. observed a decrease in Co crystallite size as the pH increased from acidic to neutral to basic which agrees with the variations in size observed in this study [27]. However, despite them using a similar synthesis procedure, the Co crystallite sizes they reported (at pH 2) were larger than those observed here. The smaller values obtained in this study may derive from Co passivation required for XRD analysis and assumptions used in estimating the values from the H_2-TPD results. Passivation may shrink the metallic Co component (core) of the crystallite by one or two atom layers which will reduce the size estimated from the XRD peaks. Size estimates based on the H_2-TPD results assume the Co is completely reduced. Earlier work [24] showed the reduction protocol applied to these samples reduced approximately ~80% of the Co on the surface in which case the calculation of the Co crystallite size may also be an underestimate.

Methanation activity of the catalyst samples, in terms of CO conversion, is provided in Fig. 5. Catalysts prepared using the non-aqueous process exhibited higher CO activity than their aqueous counterparts. The absolute improvement in CO conversion for the non-aqueous samples was between 7 and 8% for both γ-alumina supports. The increase in catalytic activity can be primarily attributed to the higher Co metal dispersion achieved by the non-aqueous synthesis method (as demonstrated in Fig. 6) and, to a lesser extent, the decreased presence of mixed Co species (e.g. Co aluminates) as presented in Fig. 2. To further confirm the controlling influence of Co dispersion on methanation activity CO conversion versus Co dispersion data for Co-only-promoted Norton γ-alumina (aqueous preparation – from our earlier work [24]) and Puralox γ-alumina promoted with Co alone (non-aqueous preparation) has been provided in Table 5. These catalysts exhibit low Co dispersion and a correspondingly lower methanation activity, further supporting the notion that Co dispersion is a dominant factor governing catalyst performance. Fig. 5 also indicates methanation activity is improved for the Puralox support compared with the Norton support, irrespective of the impregnation solution. Sodium content has been previously reported [38] to influence catalyst activity although the two supports in this work possessed similar Na levels (Table 1) indicating this is not the case here.

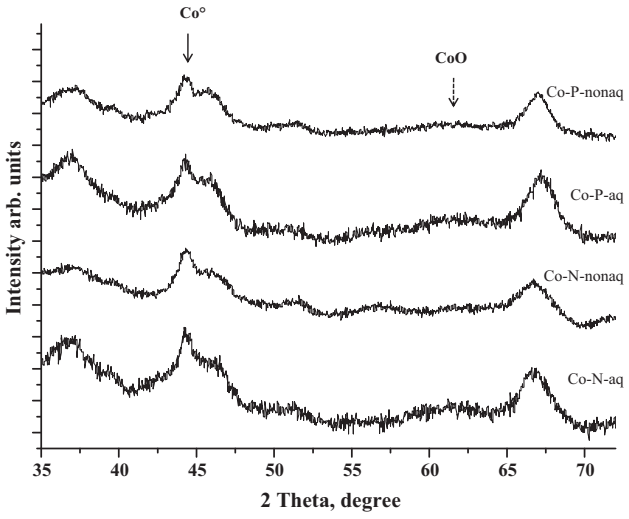

Fig. 4. X-ray diffraction patterns of alumina-supported La/Co/Ru catalysts following reduction in 50% H_2/He at 400 °C and passivation in 0.5% O_2/He at room temperature for 10 h.

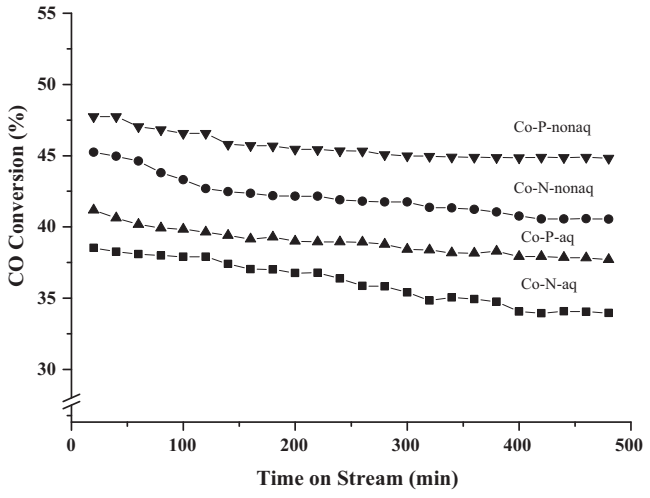

Fig. 5. CO conversion with time during the CO methanation reaction by alumina-supported La/Co/Ru catalysts impregnated using aqueous or non-aqueous precursor solutions. Catalysts were reduced in 50% H_2/He at 400 °C for 10 h prior to the methanation reaction. Conditions during methanation were reactant gas ratio (H_2/CO) = 10, flow rate = 50 ml/min, temperature = 200 °C.

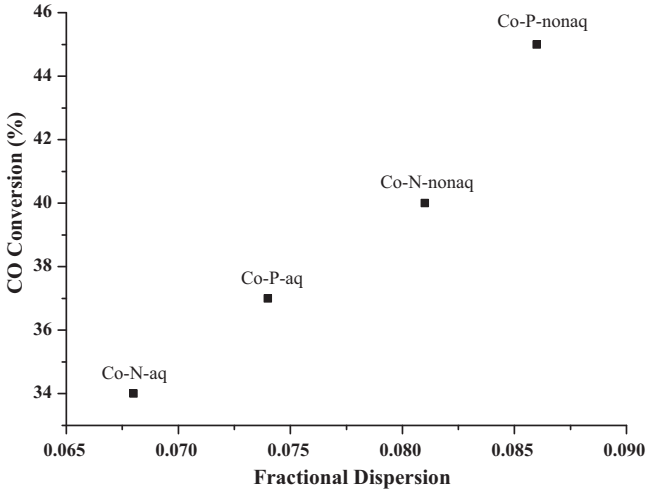

Fig. 6. Relationship between Co metal dispersion and CO conversion during the methanation reaction by alumina-supported La/Co/Ru catalysts.

Table 5
Relationship between Co metal dispersion and CO conversion during the methanation reaction by alumina-supported La/Co/Ru catalysts.

Sample	CO conversion (%)	Fractional Co dispersion
Co/P-nonaq[a]	19	0.055
Co/N-aq[b]	24	0.059
Co-P-aq	34	0.068
Co-N-aq	37	0.074
Co-P-nonaq	40	0.081
Co-N-nonaq	45	0.086

[a] Corresponds to Puralox γ-alumina promoted with Co alone.
[b] Corresponds to Norton γ-alumina promoted with Co alone (taken from [24]).

Consequently, the differences in performance between the two γ-alumina supports appear to derive primarily from differences in the pore structure and the potential influence this has on Co crystallite size.

4. Conclusion

The influence of impregnation solution and support on the methanation activity of cobalt/ruthenium/lanthanum promoted γ-alumina was studied. Synthesis using a non-aqueous impregnation solution delivered a smaller Co crystallite size as well as decreased interaction between the Co and alumina surface when compared with impregnation by an aqueous precursor solution. The smaller Co crystallite size is thought to be governed by the higher pH of the non-aqueous solution while decreased interaction between Co and the alumina is suspected to derive from surface functionalisation of the catalyst by organics from the non-aqueous mixture. The smaller Co crystallite size and ensuing higher Co dispersion was found to dominate catalyst activity for the methanation reaction.

Acknowledgement

The authors wish to thank the ARC Centre of Excellence for Functional Nanomaterials for financial support.

References

[1] R.L. Palmer, D.A. Vroom, J. Catal. 50 (1977) 244.
[2] A. Ignatiev, T. Matsuyama, J. Catal. 58 (1979) 328.
[3] J. Ojewska, R. Dziembaj, J. Mol. Catal. A 122 (1997) 1.
[4] H.P. Withers Jr., K.F. Eliezer, J.W. Mitchell, Ind. Eng. Chem. Res. 29 (1990) 1807.
[5] G. Jacobs, T.K. Das, Y. Zhang, J. Li, G. Racoillet, B.H. Davis, Appl. Catal. A–Gen. 233 (2002) 263.
[6] J.M. Zowtiak, C.H. Bartholomew, J. Catal. 83 (1983) 107.
[7] H. Schaper, E.B.M. Doesburg, P.H.M. De Korte, L.L. Van Reijen, Appl. Catal. 14 (1985) 371.
[8] M.A. Vannice, C. Sudhakar, M. Freeman, J. Catal. 108 (1987) 97.
[9] T.K. Das, G. Jacobs, P.M. Patterson, W.A. Conner, J. Li, B.H. Davis, Fuel 82 (2003) 805.
[10] R. Oukaci, A.H. Singleton, J.G. Goodwin, Appl. Catal. A–Gen. 186 (1999) 129.
[11] D. Schanke, S. Vada, E.A. Blekkan, M.A. Hilmen, A. Hoff, A. Holmen, J. Catal. 156 (1995) 85.
[12] E. Iglesia, S.L. Soled, R.A. Fiato, J. Catal. 137 (1992) 212.
[13] B.G. Johnson, C.H. Bartholomew, D.W. Goodman, J. Catal. 128 (1991) 231.
[14] W.H. Lee, C.H. Bartholomew, J. Catal. 120 (1989) 256.
[15] Y. Zhang, Y. Liu, G. Yang, Y. Endo, N. Tsubaki, Catal. Today 142 (2009) 85.
[16] S.W. Ho, Y.S. Su, J. Catal. 168 (1997) 51.
[17] A.F. Lucredio, J.D.A. Bellido, A. Zawadzki, E.M. Assaf, Fuel 90 (2011) 1424.
[18] A. Sirijaruphan, A. Horvath, J.G. Goodwin, R. Oukaci, Catal. Lett. 91 (2003) 89.
[19] S.L. Soled, J.E. Baumgartner, S.C. Reyes, E. Iglesia, Mater. Res. Soc. Symp. Proc. 368 (1995) 113.
[20] Y. Zhang, Y. Liu, G. Yang, S. Sun, N. Tsubaki, Appl. Catal. A – Gen. 321 (2007) 79.
[21] S.W. Ho, M. Houalla, D.M. Hercules, J. Phys. Chem. 94 (1990) 6396.
[22] H. Ming, B.G. Baker, Appl. Catal. A – Gen. 123 (1995) 23.
[23] K.M. Hardiman, C.H. Hsu, T.T. Ying, A.A. Adesina, J. Mol. Catal. A – Chem. 239 (2005) 41.
[24] E. Kok, J. Scott, N. Cant, D. Trimm, Catal. Today 164 (2011) 297.
[25] T.P. Kobylinski, C. L. Kibby, R.B. Pannell, A. Park, E.L. Eddy. U.S. Patent 4,605,676 (1986).
[26] E. Rytter, S. Eri, International Publication Number WO 2006/010936 A1 (2006) to Statoil ASA and PetroSA.
[27] J.W. Bae, Y.J. Lee, J.Y. Park, K.W. Jun, Energy Fuels 22 (2008) 2285.
[28] H. Xiong, Y. Zhang, S. Wang, J. Li, Catal. Commun. 6 (2005) 512.
[29] S. Bateson, Vacuum 2 (1952) 365.
[30] W. Chu, P.A. Chernavskii, L. Gengembre, G.A. Pankina, P. Fongarland, A.Y. Khodakov, J. Catal. 252 (2007) 215.
[31] J. Hong, P.A. Chernavskii, A.Y. Khodakov, W. Chu, Catal. Today 140 (2009) 135.
[32] P. Basu, D. Panayotov, J.T. Yates, J. Am. Chem. Soc. 110 (1988) 2074.
[33] E.C. Decanio, V.P. Nero, J.W. Bruno, J. Catal. 135 (1992) 135.
[34] A. Taylor, R.W. Floyd, Acta Crystallogr. 3 (1950) 285.
[35] G. Natta, M. Strada, Gazz. Chim. Ital. 58 (1928) 419.
[36] G. Will, N. Masciocchi, W. Parrish, M. Hart, J. Appl. Chem. 20 (1987) 394.
[37] A.Y. Khodakov, W. Chu, P. Fongarland, Chem. Rev. 107 (2007) 1692.
[38] O. Borg, S. Eri, E.A. Blekkan, S. Storsaeter, H. Wigum, E. Rytter, A. Holmen, J. Catal. 248 (2007) 89.